International Journal of Latest Research in Science and Technology **ISSN (Online):2278-5299**
Volume 13, Issue 2: Page No.1-10 (2024)
https://www.mnkjournals.com/journal/ijlrst/index.php

Identifying Highly Reactive Nanoplastic Polymers Using Frontier Molecular Orbital Theory and Computationally Modeling Associated Cellular Uptake of Modified Nanopolymers in Gastrointestinal Environments

Aryaman Tiwary[1*], Dr. Somnath Mukhopadhyay[2]
Additional Research Supervisors: Mr. Robert Gotwals[3] and Dr. Sarah Shoemaker[3]
[1] Raleigh Charter High School, Cary, North Carolina.
Email: atiwary@raleighcharterhs.org, United States of America
[2]North Carolina Central University, Biomedical and Biotechnology Research Institute, Durham, North Carolina.
Email: smukhopadhyay@nccu.edu, United States of America
[3]North Carolina School of Science and Mathematics SRIP, Durham, North Carolina, United States of America

Received: 15 September 2024; Accepted: 4 October 2024; Published :09 December 2024

Abstract:
Background: With recent findings revealing significant micro and nanoplastic (MNPL) concentrations in human blood samples, MNPLs have emerged as a topic of pertinence due to their cytotoxicity. In various gastrointestinal and pulmonary cells, polystyrene microbeads have been evidenced to prompt membrane depolarization and trigger cellular apoptosis, with adversariality varying by MNPL concentration, size of plastic, and presence of surface modifications. Surface modifications in particular, such as amination (R-NH2), have been qualitatively observed to enhance cellular uptake and thereby toxicity in gastrointestinal cells, while modifications such as carboxylation (R-COOH) impede uptake. However, few computational models address the effects on uptake and likelihood of surface modifications in different plastics.
Objective: This paper utilizes Frontier Molecular Orbital Theory to predict likely reactions between plastic types and common reagents. Examining HOMO-LUMO gaps can help ascertain polymer reactivity and thereby provide insights into polymer potency.
Methods: The Gaussian software with the B3LYP functional was used to make HOMO-LUMO approximations with a 6-31G(d) basis set. Next, the IBM RXN for Chemistry tool was employed to sequence plausible reaction pathways for organic synthesis. Finally, a NetLogo Henderson-Hasselbach transmembrane migration model was used to confirm the effects of carboxylation and amination on membrane penetration of nanopolymers. pKa values for drug migration were modeled in Gaussian using the M06 suite of functionals with a more accurate 6-311+G(2d,p) basis set solvated in water.
Results: Among 9 plastic types, ethylene propylene diene and polypropylene polymers were the most reactive and likely to acquire surface modifications. Next, to examine reaction plausibility, retrosynthetic simulations with certain parameters revealed over 30 plausible sequences for each type of carboxyl and amine functionalization for polypropylene and only 1 plausible sequence for each modification of ethylene propylene diene. Finally, to validate the qualitative findings regarding uptake, transmembrane motion of polypropylene with different functionalizations was modeled using the computationally determined polypropylene pKa values–9.9 and 45.6 for carboxylated and aminated polypropylene, respectively–and the Henderson-Hasselbach drug migration model. This model confirmed that carboxylation impedes cellular uptake while amination enhances uptake in various gastrointestinal environments, ranging in pH from 5.7 to 7.4.

***Keywords*:** Frontier Molecular Orbital Theory; Nanoplastics and cellular uptake; Plastics and surface modifications; Computational Chemistry.

1. INTRODUCTION

Overview of Plastic Production and Prevalence

Plastics are long polymer chains derived from hydrocarbon mixtures such as crude oil (1). These mixtures are separated into their components via fractional distillation, with plastic progenitors like ethane and propane possessing lower boiling points of -89 °C and -42 °C respectively (2). The aforementioned components then undergo cracking to form plastic monomers like ethylene and propylene, which are conjoined via processes like addition polymerization or condensation polymerization to long-chain polymers (3). These synthetic chains are later combined with various additives like phthalates, flame retardants, and BPA to enhance favorable characteristics like flexibility, resistance to combustion, and durability (3). Plastics have a high strength-to-weight ratio, making them useful across industries: as

drippers and nozzles in irrigation systems, packaging for consumer and edible goods, piping and insulation in buildings, single-use medical packaging, and in automotives to make cars lighter (4). To allow for such versatility in utilization, multiple plastic types exist for different purposes, such as Polyethylene (PE), Polyethylene Terephthalate (PET), Polyvinyl Chloride (PVC), Polypropylene (PP), and Polystyrene (PS) to name a few. With a global market size of over $624.16 billion (as estimated in 2023), plastics are particularly prevalent in modern society with an established niche encompassing industries (4). However, with this utility comes a physiological cost. Recently published medical literature highlights the potential drawbacks that accompany widespread adoption of plastics; the primary issue presents in smaller plastics referred to as micro or nanoplastics that are proliferating into human systems.

Emergence of Micro and Nanoplastics (MNPLs) in the Environment

Nanoplastics are defined as plastic particles ranging from 1 nanometer (nm) in diameter to 100 nm (5). Their larger counterparts, microplastics, are not rigidly defined in terms of diameter, but it is generally accepted that microplastics are plastic particles with diameters ranging from 1 micrometer to 5 millimeters (5). Primary micro and nanoplastics (MNPLs) are those produced for intentional use, typically in cosmetic exfoliants, nurdles that are manufactured into larger products at facilities, microfibers in clothes, and drug delivery systems (6). However, as revealed by an examination of water bodies surrounding Europe, intentionally produced MNPLs comprise a minority of those polluting aquatic systems (7). The majority at hand here are secondary MNPLs–unintentionally produced micro or nanoplastics that are the result of plastic degradation (7). Larger plastics exposed to physical wear and tear, wind erosion, extended periods of UV radiation, certain microorganisms, or oxidative chemicals can all contribute to the production of secondary MNPLs (6).

MNPL Exposure in Humans

Recent findings reveal that not only are these MNPLs polluting ecosystems but significant micro and nanoplastic concentrations have been detected in human blood–a study on blood donors estimates this figure as between 1.84-4.65 micrograms of plastic/mL of blood collected (6). The most common types of plastics found in this study were polyethylene (32% of plastic in a given blood sample), ethylene propylene diene (14%), and ethylene vinyl acetate (12%) (6). However, qualitative findings regarding MNPLs have only focused on polystyrene (micro)beads functionalized with various groups, even though polystyrene proliferation is only one of the problematic polymer types. Though difficult to accurately determine, data has been collected to estimate the sources from which humans are ingesting microplastics. The following image is taken from one such study coalescing reliable data to make novel predictions:

MNPLs and Cellular Toxicity

Such data reveals that significant MNPL exposure is a byproduct of excessive plastic use and disposal, and, so, the adversariality of MNPL exposure to human health has emerged as a pertinent issue to address. Reviews authored by Dr. Banerjee and Dr. Shelver examine the mechanisms of cytotoxicity elicited by microplastics along with other factors that either exacerbate toxicity or impede MNPL associated damages.

Exposure-pathway	Product	Recommended-estimated consumption	Mean MNPLs	Daily intake of MNPLs	Annual intake of MNPLs	Total MNPLs/year
Ingestion	Fruit and vegetables	400g/day	132740p/g	53.09×10^{6}	19.38×10^{9}	2.93×10^{10}
	Seafood	22.41kg/year	0.98p/g	60.38	22.04×10^{3}	
	Bottled water	2L/day	13.55×10^{6}p/L	27.10×10^{6}	9.89×10^{9}	
	Salt	5g/day	142.80p/kg	0.71	260.61	
	Alcohol	6.40L/year	4.05p/L	0.07	25.92	
Inhalation	Air	$8.64m^3$/day	$0.68p/m^3$	5.92	2.16×10^{3}	2.16×10^{3}

(5) p/g represents particles per gram.

As expected, the dosage required for cytotoxic effects to manifest depends significantly on factors like the type of cell examined, size of plastics, presence of surface modifications, exposure time, with cytotoxic thresholds varying from a few micrograms of plastic/mL of blood to a few hundred micrograms/mL for polystyrene microbeads. The mechanism of cytotoxicity, prompted by membrane disruption caused by polystyrene exposure and eventually leading to the activation of a caspase transduction pathway for cellular apoptosis, is best illustrated by the following graphic and description from the Banerjee and Shelver review.

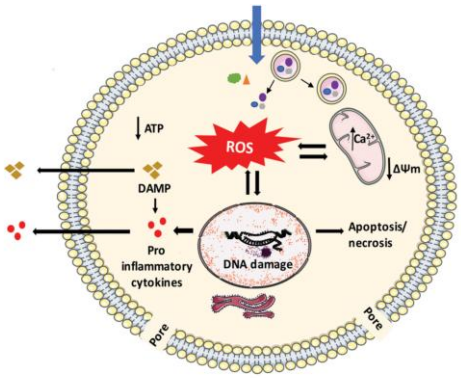

Fig. 4. Plausible mechanisms of cytotoxicity induced by micro/nanoplastics. Uptake of micro- or nanoplastics can lead to loss in plasma/endo-lysosomal/nuclear membrane integrity causing pore formation in the membranes and subsequent reactive oxygen species (ROS) generation from the mitochondria. Increased levels of intracellular ROS can cause mitochondrial damage due to increase in mitochondrial Ca^{2+}, concomitant mitochondrial membrane depolarization (↓ΔΨm), release of pro-apoptotic factors from the mitochondria, reduction in ATP, release of damage associated molecular patterns (DAMP) from mitochondria or other organelles, consequent production/release of pro-inflammatory cytokines and finally activation of cell death pathways leading to apoptosis or necrosis. All these processes are intricately inter-connected, therefore induction of one process can lead to activation of other processes.

(8)

Research Questions and Study Objectives

One persistent theme throughout current experimentally derived literature is that certain surface modifications, such as carboxyl (COOH) or amine (NH_2) functionalizations, significantly affect uptake of microplastics into cell membranes, as observed qualitatively in gastrointestinal environments (ranging in pH from 5.7 to 7.4–see *Materials and Methods*) (8). However, there are few computational models to describe the characteristics of reactions involving microplastics, product stabilities, and cellular uptake. The following research questions highlight the objectives of the paper: Which plastic types are the most reactive and likely to acquire surface modifications? What are the mechanisms of these "most likely" reactions, and are they plausible in real conditions with restricted compound availability and

environmental conditions? How do these surface modifications affect cellular uptake in gastrointestinal environments as modeled computationally?

The approach presented in this paper involves the utilization of computational chemistry tools such as Gaussian to employ Frontier Orbital Molecular Orbital Theory (FMOT) and predict likely reactions between plastics and various functional group containing molecules. FMOT focuses particularly on HOMO-LUMO interactions between and within molecules. In this context, HOMO and LUMO are acronyms for "Highest Occupied Molecular Orbital" and "Lowest Occupied Molecular Orbital" respectively. A smaller gap in the energy of electrons in the HOMO of one molecule and electrons in the LUMO of another indicates higher reaction favorability (9). Additionally, a smaller gap in the energy of electrons in the HOMO and LUMO of the same molecule indicates lower stability and higher reactivity (9).

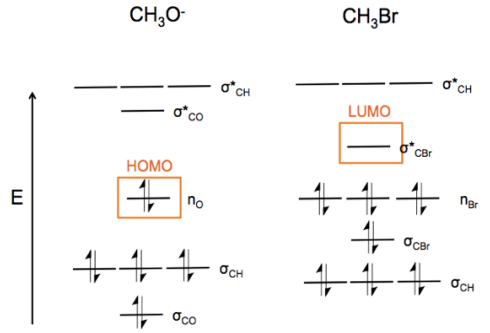

(10)

The project also addressed practical plausibility of microplastic functionalization through AI aided simulations taking certain constraints into account. Finally, the Henderson-Hasselbach equation was used to model transmembrane movement of functionalized microplastics in different gastrointestinal environments.

The Henderson-Hasselbach equation relates the pH of an environment to the pKa (-log base 10 of the acid dissociation constant of a given species) of the primary reacting species, taking into consideration the concentrations of the protonated and deprotonated forms of the species present.

2. METHODS

HOMO and LUMO energies of respective molecules and electrostatic potential maps displaying regional electron densities were obtained using the Gaussian tool for chemistry, which makes use of Gaussian functions to make approximations including energy of electron correlation, kinetic energy, and potential energy. For this part of the project, the B3LYP functional was used to make the aforementioned approximations with a 6-31G(d) basis set (6: six Gaussian functions to describe the core (inner) electrons. 3: three Gaussian functions to describe the inner part of the valence electrons. 1: one Gaussian function to describe the outer part of the valence electrons). These settings were used to make calculations relating to Molecular Orbitals and balance computational efficiency and accuracy. HOMO-LUMO approximations in hartrees (au) were performed for the following problematic plastic types and common functionalization species (with common species and their structures obtained from various papers and manually modeled in Gaussian): *Styrene (monomer), Ethylene (monomer), Propylene (monomer) Polystyrene (3 units), Polyethylene (3 units), Polypropylene (3 units), Ethylene propylene diene (3 units), Ethylene vinyl acetate (3 units), Polyethylene terephthalate (3 units), Sodium Lauryl Sulfate, Vitamin E (TPGS), 4-(N-methyltetrahydropyrimidine)benzyl alcohol (amidine containing), N- (Bromomethyl)phthalimide (amine containing), Acrylic acid (carboxyl containing), Succinic acid (carboxyl containing), Amidine, Amine, Carboxyl, and Hydroxyl* (13,14,15,16,17,18). Polymer lengths were limited to 3 subunits in order to preserve computational efficiency.

$$pH = pk_A + \log_{10} \frac{[\text{conjugate base}]}{[\text{weak acid}]} \quad (11)$$

HOMO-LUMO Data		
Molecule	HOMO	LUMO
Styrene (monomer)	-0.219	-0.03
Ethylene (monomer)	-0.266	0.0172
Propylene (monomer)	-0.249	0.0269
Sodium Lauryl Sulfate	-0.165	-0.143
Carboxyl group	-0.292	-0.0031
Amine (NH2)	-0.247	0.079
Vitamin E (TPGS)	-0.20768	-0.00437
Hydroxyl group	0.162	0.4171
Amidine	-0.16551	-0.00638
(Amine cont.) N-(Bromomethyl)phthalimide	-0.25648	-0.08037
(carboxyl cont.) Acrylic Acid	-0.28621	-0.06845
Polystyrene (3)	-0.23649	0.00881
Polyethylene (3)	-0.29994	0.08656
Polypropylene (3)	-0.14141	-0.07148
Succinic Acid	-0.29669	-0.01295
(Amidine containing) 4-(N-methyltetrahydropyrimidine)benzyl alcohol	-0.2087	-0.01468
ethylene propylene diene (3)	-0.13294	-0.07112
PET	-0.24743	-0.08337
ethylene vinyl acetate	-0.16813	-0.0481
PET (3)	-0.25129	-0.09026

Next, to algorithmically sort inter and intramolecular HOMO-LUMO gaps (HOMO energy - LUMO energy), Mathematica was used to organize and sort the data into a table following a recursive sorting algorithm that determined the likelihood of every reaction possible with the aforementioned molecules for which the HOMO-LUMO energies (in hartrees) were obtained.

```
dataList = {}
For[i = 2, i ≤ 21, i++, tempHOMO = homo[i];

 For[b = 2, b ≤ 21, b++, tempLUMO = lumo[b];

  tempDifference = tempHOMO - tempLUMO;

  dataList2 = {molecule[i], molecule[b], tempDifference};
  If[And[molecule[i] == "Styrene (monomer)" || molecule[i] == "Ethylene (monomer)" || molecule[i] == "Propylene (monomer)" || molecule[i] == "Polystyrene (3)" ||
     molecule[i] == "Polyethylene (3)" || molecule[i] == "Polypropylene (3)" || molecule[i] == "ethylene propylene diene (3)" || molecule[i] == "PET" ||
     molecule[i] == "PET (3)" || molecule[i] == "ethylene vinyl acetate" || molecule[b] == "Styrene (monomer)" || molecule[b] == "Ethylene (monomer)" ||
     molecule[b] == "Propylene (monomer)" || molecule[b] == "Polystyrene (3)" || molecule[b] == "Polyethylene (3)" || molecule[b] == "Polypropylene (3)" ||
     molecule[b] == "ethylene propylene diene (3)" || molecule[b] == "PET" || molecule[b] == "PET (3)" || molecule[b] == "ethylene vinyl acetate"],
   AppendTo[dataList, dataList2],
      Null

  ]
 ]

]

sortedDataList = SortBy[dataList, Abs[#[3]] &];
Print[dataList];
Print[sortedDataList]
Grid[Prepend[sortedDataList, {"HOMO-LUMO Data"}], Frame → All]
```

Once the most reactive polymers, ethylene propylene diene and polypropylene, were determined the IBM RXN for Chemistry tool was utilized to develop retrosynthetic routes for the production of functionalized MNPLs. Computational efficiency was compromised to produce an exhaustive list of retrosynthetic pathways, including those constrained to starting with common reagents like acrylic acid and succinic acid for carboxylation, N-(Bromomethyl)phthalimide for amination, and 4-(N-methyltetrahydropyrimidine) benzyl alcohol for amidine functionalization. Additional constraints like temperature limits of 350 Kelvin and synthesis of significant amounts of the target molecule were also employed (minimum of 500 milligrams). Due to the reduced computational efficiency, only the two most problematic plastic polymers were analyzed for these routes.

Finally, to validate the claim of researchers regarding increased transmembrane migration of aminated MNPLs in gastrointestinal cells and reduced migration of carboxylated plastics, a NetLogo Drug Migration Model was used. The model relied on the Henderson-Hasselbach equation to make predictions regarding drug permeation.

The settings used in this context of gastrointestinal cells, included a surrounding pH of 6, 7.4, 5.7, and 6.7 to simulate the duodenum, terminal ileum, caecum, and rectum respectively and computational pKa determination of plastics from Gaussian using the change in Gibbs free energy of dissociation, which was done using the M06 suite of functionals with a more accurate 6-311+G(2d,p) basis set solvated in water to perform calculations involving vibrational frequencies ("Optimize + Vib Freq") (19).

Only the pH extrema were tested (pH = 5.7 and pH = 7.4) to derive conclusions for each type of functionalization on polypropylene (only one type of plastic tested to preserve efficiency in pKa determination). The fundamental equation of relevance used here was as follows:

$$\Delta G^{o} = -RT \ln K \quad (20)$$

G = Gibbs free energy (joules)
R = universal gas constant (8.314 joules * kelvins^{-1} * mol^{-1})
T = temperature in Kelvin
K = equilibrium constant for the given reaction.

Obtained Gibbs free energy values from Gaussian:

(Unionized) carboxylated polypropylene	-582.401461 hartrees
(Ionized) carboxylated polypropylene	-582.204462283 hartrees
Proton	-0.174563 hartrees
(Unionized) Aminated Polypropylene	-465.232024 hartrees
(Ionized) Aminated Polypropylene	-464.955312846 hartrees

Per the above data, the pKa's (negative logarithm with base 10 of the equilibrium constant above) of carboxylated and aminated polypropylene (3 units) were computationally calculated as 9.921 and 45.610 respectively. These calculations were made with respect to a human body temperature of 310.15 Kelvin, a conversion factor of 1 hartree to 4.35974 x 10^{-18} joules, and a water dissociation constant of 2.24 x 10^{-14} at this temperature (21).

3. RESULTS

The Figures that follow display the results obtained using the methodology detailed above. The following results display the reaction likelihoods of plastics and different reagents via an FMOT analysis, the plausibility of the most reactive plastics acquiring modifications through the simulation of different organic syntheses, and finally the effect of carboxylation and amination on the most reactive and potent plastic found: polypropylene.

Figure 1 - 40 plausible sequences for polypropylene amination, 30 for carboxylation, 1 plausible sequence for ethylene propylene diene (EPD) amination and carboxylation with constraints detailed in Materials and Methods. The IBM RXN for Chemistry tool interface was used to produce these results.

"HOMO-LUMO Data"		
"Polypropylene (3)"	"Sodium Lauryl Sulfate"	0.0015899999999999803`
"ethylene propylene diene (3)"	"Sodium Lauryl Sulfate"	0.010059999999999986`
"ethylene vinyl acetate"	"Sodium Lauryl Sulfate"	-0.025130000000000013`
"ethylene propylene diene (3)"	"PET (3)"	-0.042679999999999996`
"ethylene propylene diene (3)"	"PET"	-0.04957`
"Polypropylene (3)"	"PET (3)"	-0.05115`
"ethylene propylene diene (3)"	"(Amine cont.) N-(Bromomethyl)phthalimide"	-0.052570000000000006`
"Polypropylene (3)"	"PET"	-0.05804000000000001`
"Polypropylene (3)"	"(Amine cont.) N-(Bromomethyl)phthalimide"	-0.06104000000000001`
"ethylene propylene diene (3)"	"Polypropylene (3)"	-0.06146`
"ethylene propylene diene (3)"	"ethylene propylene diene (3)"	-0.06182`
"ethylene propylene diene (3)"	"(carboxyl cont.) Acrylic Acid"	-0.06449`
"Polypropylene (3)"	"Polypropylene (3)"	-0.06993`
"Polypropylene (3)"	"ethylene propylene diene (3)"	-0.07029`
"Polypropylene (3)"	"(carboxyl cont.) Acrylic Acid"	-0.07296000000000001`
"Sodium Lauryl Sulfate"	"PET (3)"	-0.07474`
"Amidine"	"PET (3)"	-0.07524999999999998`
"Hydroxyl group"	"Polyethylene (3)"	0.07544000000000001`
"Styrene (monomer)"	"Sodium Lauryl Sulfate"	-0.07600000000000001`
"ethylene vinyl acetate"	"PET (3)"	-0.07787`
"Sodium Lauryl Sulfate"	"PET"	-0.08163000000000001`
"Amidine"	"PET"	-0.08213999999999999`
"ethylene vinyl acetate"	"PET"	-0.08476`
"ethylene propylene diene (3)"	"ethylene vinyl acetate"	-0.08484`
"ethylene vinyl acetate"	"(Amine cont.) N-(Bromomethyl)phthalimide"	-0.08776`
"Polypropylene (3)"	"ethylene vinyl acetate"	-0.09331`
"Polystyrene (3)"	"Sodium Lauryl Sulfate"	-0.09349000000000002`
"Sodium Lauryl Sulfate"	"Polypropylene (3)"	-0.09352`
"Sodium Lauryl Sulfate"	"ethylene propylene diene (3)"	-0.09388`
"Amidine"	"Polypropylene (3)"	-0.09402999999999999`
"Amidine"	"ethylene propylene diene (3)"	-0.09438999999999999`
"ethylene vinyl acetate"	"Polypropylene (3)"	-0.09665`
"ethylene vinyl acetate"	"ethylene propylene diene (3)"	-0.09701`
"ethylene vinyl acetate"	"(carboxyl cont.) Acrylic Acid"	-0.09968`
"ethylene propylene diene (3)"	"Styrene (monomer)"	-0.10294`
"PET"	"Sodium Lauryl Sulfate"	-0.10443000000000002`
"Propylene (monomer)"	"Sodium Lauryl Sulfate"	-0.10600000000000001`
"PET (3)"	"Sodium Lauryl Sulfate"	-0.10829000000000003`
"Polypropylene (3)"	"Styrene (monomer)"	-0.11141000000000001`
"Sodium Lauryl Sulfate"	"ethylene vinyl acetate"	-0.1169`
"Amidine"	"ethylene vinyl acetate"	-0.11740999999999999`
"Vitamin E (TPGS)"	"PET (3)"	-0.11742`
"ethylene propylene diene (3)"	"(Amidine containing) 4-(N-methyltetrahydropyrimidine)benzyl alcohol"	-0.11826`
"(Amidine containing) 4-(N-methyltetrahydropyrimidine)benzyl alcohol"	"PET (3)"	-0.11843999999999999`
"ethylene propylene diene (3)"	"Succinic Acid"	-0.11999`
"ethylene vinyl acetate"	"ethylene vinyl acetate"	-0.12003`
"Ethylene (monomer)"	"Sodium Lauryl Sulfate"	-0.12300000000000003`
"Vitamin E (TPGS)"	"PET"	-0.12431`
"(Amidine containing) 4-(N-methyltetrahydropyrimidine)benzyl alcohol"	"PET"	-0.12533`
"ethylene propylene diene (3)"	"Amidine"	-0.12656`
"Polypropylene (3)"	"(Amidine containing) 4-(N-methyltetrahydropyrimidine)benzyl alcohol"	-0.12673`
"Polypropylene (3)"	"Succinic Acid"	-0.12846000000000002`
"ethylene propylene diene (3)"	"Vitamin E (TPGS)"	-0.12857`
"Styrene (monomer)"	"PET (3)"	-0.12874`
"ethylene propylene diene (3)"	"Carboxyl group"	-0.12984`
"Sodium Lauryl Sulfate"	"Styrene (monomer)"	-0.135`
"Polypropylene (3)"	"Amidine"	-0.13503`
"Hydroxyl group"	"Propylene (monomer)"	0.1351`
"Amidine"	"Styrene (monomer)"	-0.13551`
"Styrene (monomer)"	"PET"	-0.13563`
"Vitamin E (TPGS)"	"Polypropylene (3)"	-0.1362`
"Vitamin E (TPGS)"	"ethylene propylene diene (3)"	-0.13656000000000001`
"Polypropylene (3)"	"Vitamin E (TPGS)"	-0.13704`
"(Amidine containing) 4-(N-methyltetrahydropyrimidine)benzyl alcohol"	"Polypropylene (3)"	-0.13722`
"(Amidine containing) 4-(N-methyltetrahydropyrimidine)benzyl alcohol"	"ethylene propylene diene (3)"	-0.13757999999999998`
"ethylene vinyl acetate"	"Styrene (monomer)"	-0.13813`
"Polypropylene (3)"	"Carboxyl group"	-0.13831000000000002`
"Styrene (monomer)"	"(Amine cont.) N-(Bromomethyl)phthalimide"	-0.13863`
"ethylene propylene diene (3)"	"Polystyrene (3)"	-0.14175000000000001`
"Hydroxyl group"	"Ethylene (monomer)"	0.1448`
"Polystyrene (3)"	"PET (3)"	-0.14623`
"Styrene (monomer)"	"Polypropylene (3)"	-0.14751999999999998`
"Styrene (monomer)"	"ethylene propylene diene (3)"	-0.14788`
"ethylene propylene diene (3)"	"Ethylene (monomer)"	-0.15014`
"Polypropylene (3)"	"Polystyrene (3)"	-0.15022000000000002`
"Styrene (monomer)"	"(carboxyl cont.) Acrylic Acid"	-0.15055000000000002`
"Polystyrene (3)"	"PET"	-0.15312`
"Hydroxyl group"	"Polystyrene (3)"	0.15319`

Figure 2 - Reaction likelihoods between common plastic types (monomer and polymer forms included) and common reagents/functional groups obtained from various papers (in *Materials and Methods)*. The most likely reactions are at the top of the table with the smallest intermolecular HOMO-LUMO gaps (rightmost column), per data from Gaussian with parameters detailed in *Materials and Methods.* The data displayed in Mathematica represents some of the most likely reactions from 301 simulated reactions between common plastics and reagents/functional groups.

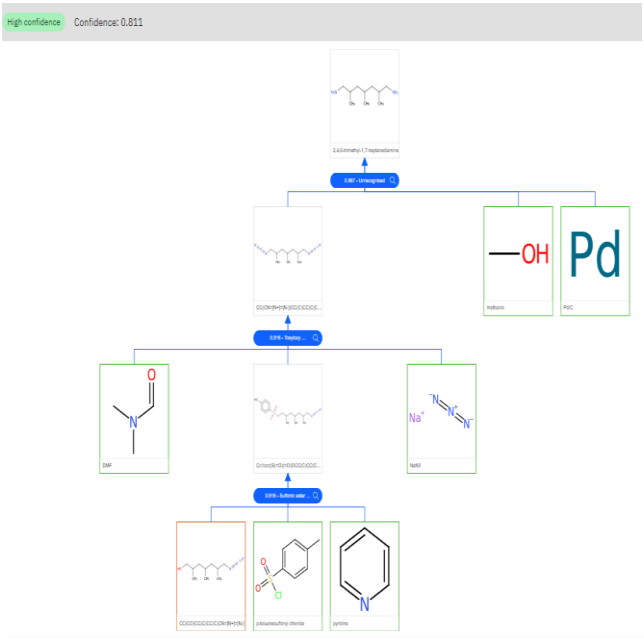

Sequence 0, Confidence: 0.811364665724359

Step 1

Type: Unrecognised, Confidence: 0.967

CC(CN=[N+]=[N-])CC(C)CC(C)CN=[N+]=[N-].CO.[Pd]>>NCC(CC(CC(CN)C)C)C

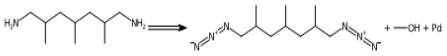

Step 2

Type: Tosyloxy N-alkylation, Confidence: 0.916

CN(C)C=O.Cc1ccc(S(=O)(=O)OCC(C)CC(C)CC(C)CN=[N+]=[N-])cc1.[N-]=[N+]=[N-].[Na+]>>CC(CN=[N+]=[N-])CC(C)CC(C)CN=[N+]=[N-]

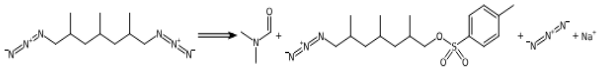

Step 3

Type: Sulfonic ester Schotten-Baumann, Confidence: 0.916

CC(CO)CC(C)CC(C)CN=[N+]=[N-].Cc1ccc(S(=O)(=O)Cl)cc1.c1ccncc1>>Cc1ccc(S(=O)(=O)OCC(C)CC(C)CC(C)CN=[N+]=[N-])cc1

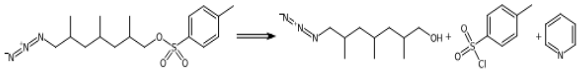

Figure 3 - Example of high confidence polypropylene amination sequence (steps in reverse order).

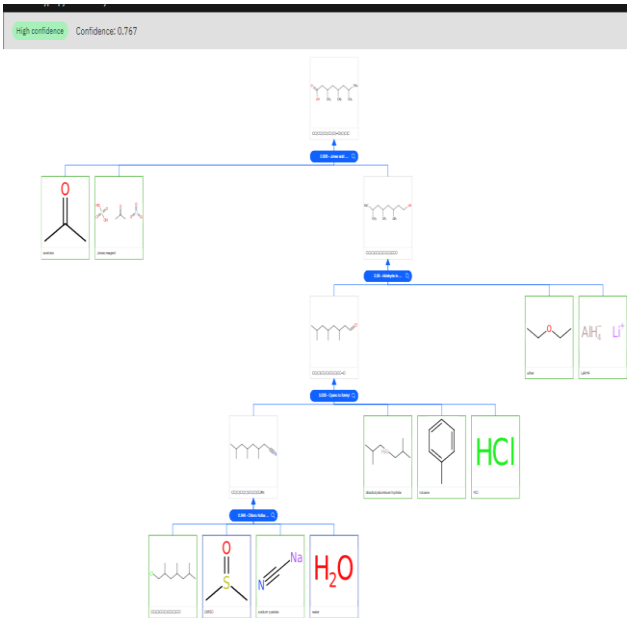

Sequence 0, Confidence: 0.7677940616136388

Step 1

Type: Jones acid oxidation, Confidence: 0.908

CC(C)=O.CC(C)=O.O=S(=O)(O)O.O=[Cr](=O)=O.CC(C)CC(C)CC(C)CCO>>CC(CC(CC(CC(O)=O)C)C)C

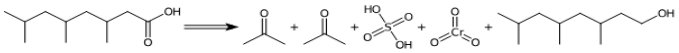

Step 2

Type: Aldehyde to alcohol reduction, Confidence: 0.95

CC(C)CC(C)CC(C)CC=O.CCOCC.[AlH4-].[Li+]>>CC(C)CC(C)CC(C)CCO

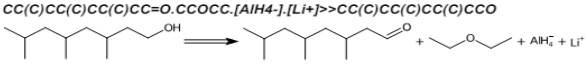

Step 3

Type: Cyano to formyl, Confidence: 0.938

CC(C)CC(C)CC(C)CC#N.CC(C)C[AlH]CC(C)C.Cc1ccccc1.Cl>>CC(C)CC(C)CC(C)CC=O

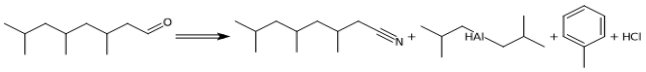

Step 4

Type: Chloro Kolbe nitrile synthesis, Confidence: 0.948

CC(C)CC(C)CC(C)CCl.CS(C)=O.N#C[Na].O>>CC(C)CC(C)CC(C)CC#N

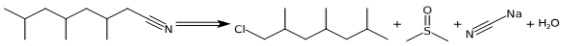

Figure 4 - Example of high confidence polypropylene carboxylation sequence (steps in reverse order).

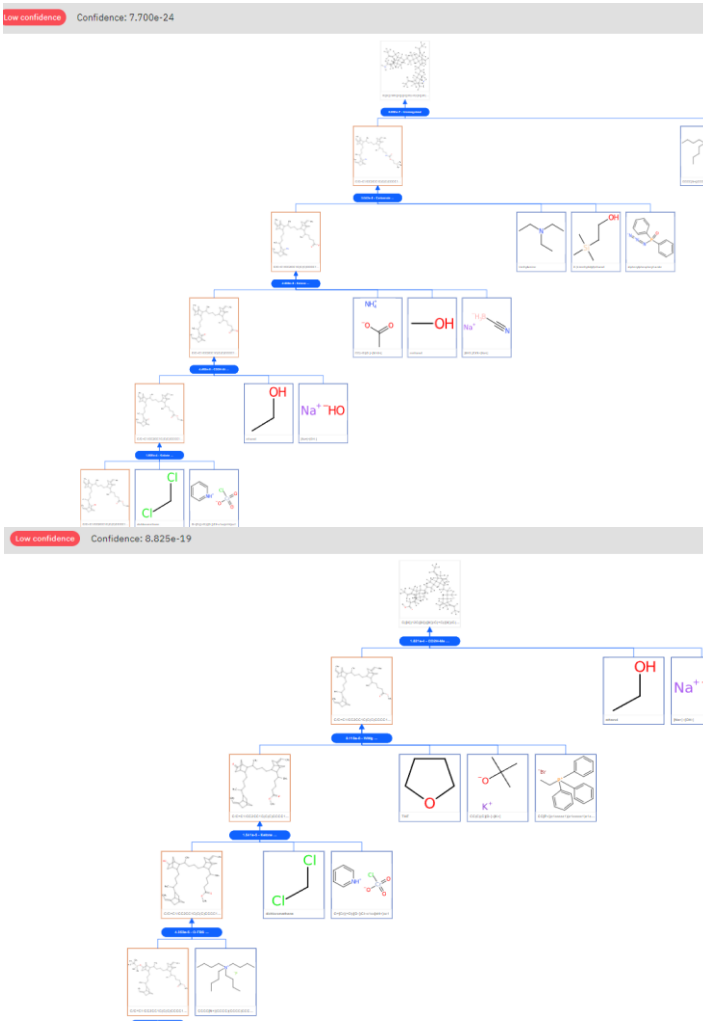

Figure 5 - Low confidence ethylene propylene diene amination and carboxylation sequences.

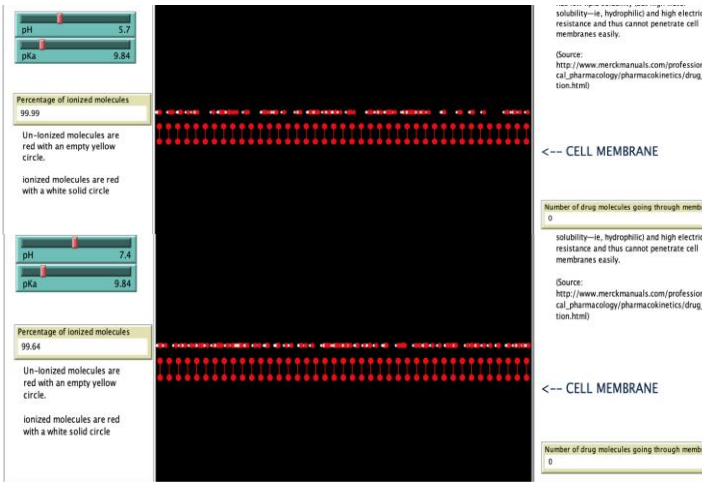

Figure 6 - Carboxylated polypropylene (pKa = 9.921, COOH–pKa determined computationally in *Materials and Methods*) does not permeate through the cell membrane in its ionized form at either gastrointestinal pH extrema (5.7 left and 7.4 right). Model only allows for pKa tuning by intervals of 0.4. Uses Henderson-Hasselbach equation.

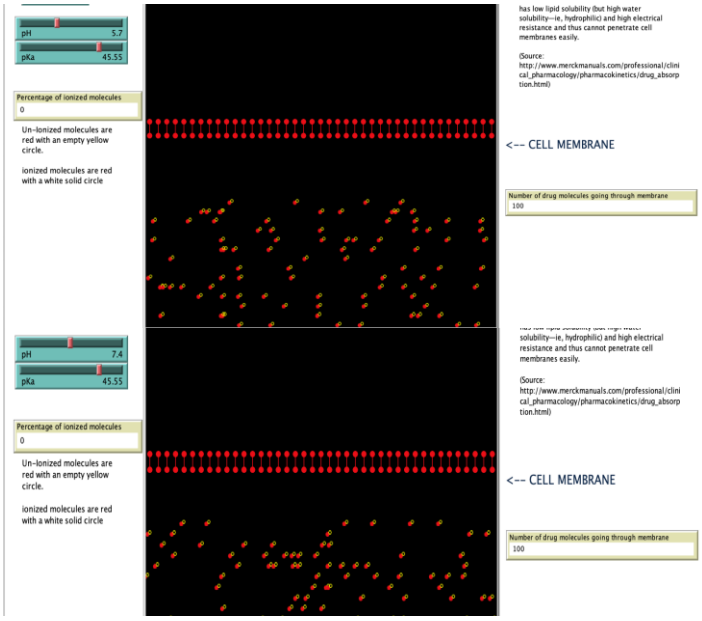

Figure 7 - Superior membrane permeation by aminated polypropylene (pKa = 45.610, NH_2) at both gastrointestinal extrema (5.7 left and 7.4 right).

4. DISCUSSION

The data table displaying reaction likelihoods (Figure 2) per the principles of FMOT reveals that plastic polymers like ethylene propylene diene and polypropylene are particularly problematic in terms of their reactivity with common functionalization species and groups, followed by polyethylene terephthalate and ethylene vinyl acetate. Additionally, these two polymers (polypropylene and ethylene propylene diene) have small intramolecular HOMO-LUMO gaps, which is indicative of their increased reactivity (<1.30) (9). This finding is particularly concerning given the significant concentrations of ethylene propylene diene found in donor blood samples (see *Introduction*). Additionally, because both plastic monomers and their polymers exhibited similar relative trends, it may be assumed that the results shown in the data table relatively sorting reaction likelihoods can be used as valid relative approximations for larger plastic polymers (larger than 3 subunits).

The simulated retrosynthetic routes (Figure 1) reveal the plausibility of MNPL functionalization. Each type of functionalization, carboxyl and amine, produced at least thirty retrosynthetic routes for polypropylene with the given constraints detailed in *Materials and Methods*, making the finding particularly problematic. However, the same functionalizations were more difficult to induce in ethylene propylene diene, with one plausible pathway for each type of functionalization. Yet, it is pertinent to note that even the intermediates within these reactions significantly alter the dipole moment of these plastics, thereby increasing the potential for membrane disruption; even if complete functionalization does not occur, any reactions can increase uptake and toxicity, therefore ethylene propylene diene proliferation is still a cause for concern. For instance, partially (positive) charged poles of plastics produced from these given "intermediary" reactions can better diffuse across a cellular membrane per the findings regarding charge uptake (8). This

behavior can be attributed to the partial negative charge of the outward facing phosphate head in the phospholipid membrane (cell membrane) attracting cationic particles and subsequently prompting membrane depolarization. For instance, the following figures display the predicted effect on charge based uptake with two modified plastic types, (ionized) aminated polypropylene and an arbitrarily selected second step intermediate within a high-confidence retrosynthetic pathway for amine functionalization of polypropylene (to preserve computational efficiency).

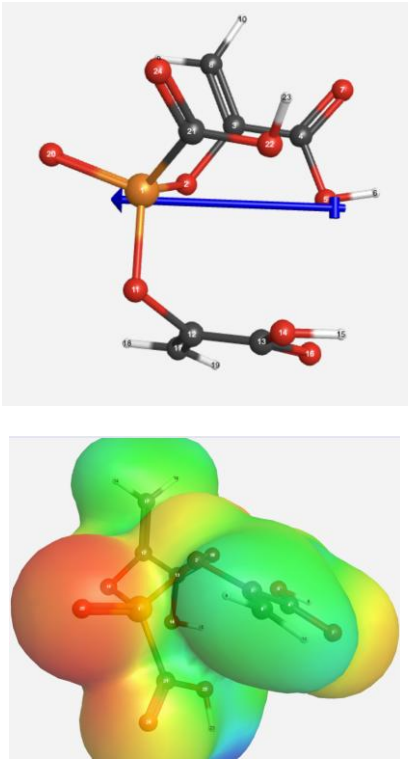

Figure 8 - A phospholipid has a significant dipole moment (blue arrow), with the electron-rich phosphate head (region in red) facing out towards foreign substances entering the cell, such as MNPLs.

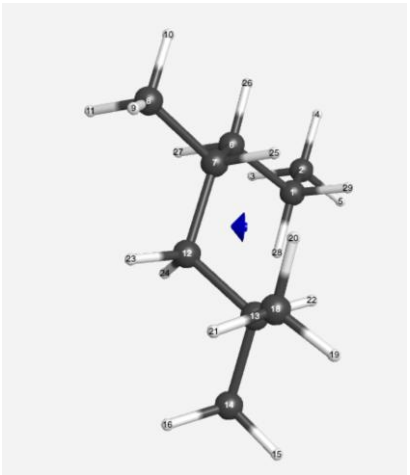

Figure 9 - Polypropylene has almost no dipole moment (blue arrow length), electron distribution is even throughout the molecule–no particular sites of attraction or repulsion with a phospholipid molecule.

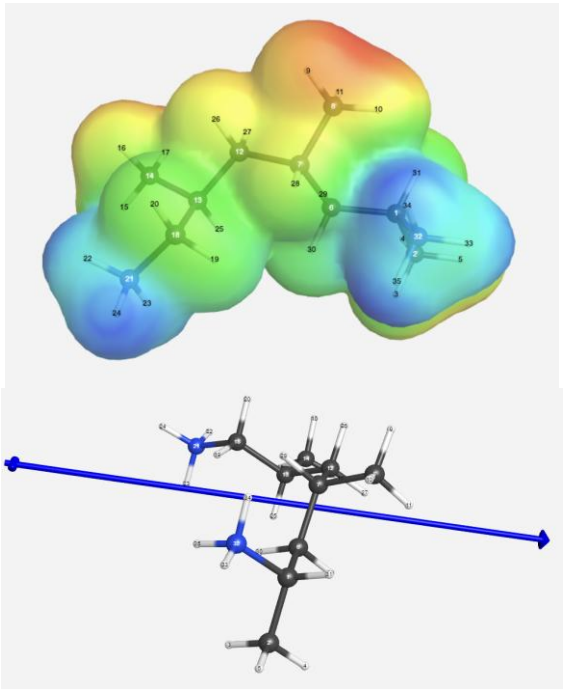

Figure 10 - (+ Ionized) Aminated Polypropylene has a significant dipole moment. The electron poor amine groups (blue region) would be attracted to the phosphate head in the phospholipid, hence cationic charges, partial or complete, enhance cellular uptake and prompt membrane depolarization–a trend mentioned in the Banerjee and Shelver review.

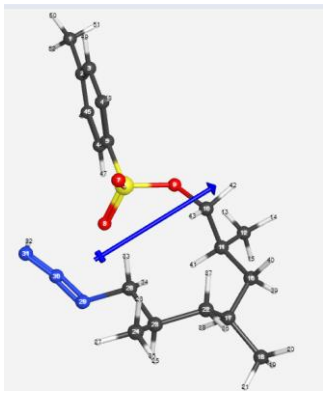

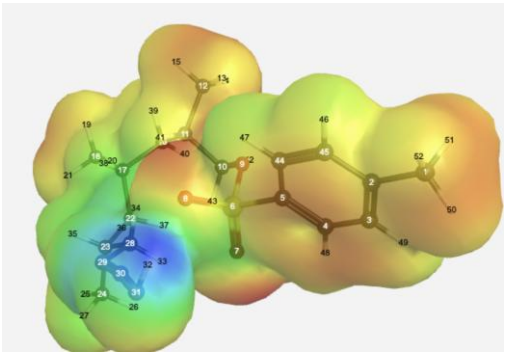

Figure 11 - Even an arbitrary second step intermediate in amine functionalization acquires a significant dipole moment with electron deficient regions that would aid in uptake.

The images above reveal that the outward facing phosphate head of the phospholipid has a partial negative charge (long arrow and electron rich red zone) that would attract the electron deficient regions in molecules with partial or complete cationic charges, such as ionized aminated polypropylene. Any reactions that alter electron distribution and induce significant electron deficient regions (exemplified best with cationic molecules) within a plastic can thereby enhance charge-based uptake. Conversely, using the same reasoning, anionic molecules would impede charge-based uptake; for instance, (ionized) carboxylated polypropylene.

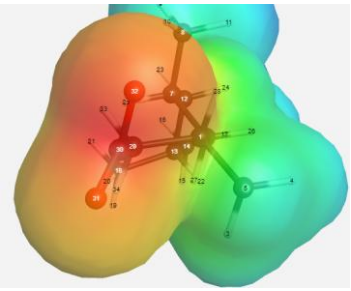

Figure 12 - (-) Carboxylated polypropylene's electron rich functional site would impede charge-based uptake.

Finally, the findings from the NetLogo drug migration model (Figures 6 & 7) validate the qualitative observations made by the researchers in the Banerjee and Shelver review (8). Per the computationally calculated pKa of 9.921 for carboxylated polypropylene, the plastic in question did not permeate through the cell membrane in its ionized form within different gastrointestinal environments detailed in *Materials and Methods* (duodenum, terminal ileum, caecum, and rectum), thereby validating the researchers' qualitative observations (8). Conversely, per the computationally calculated pKa of 45.610 for aminated polypropylene, the modified plastics easily permeated through the cell in gastrointestinal environments as predicted.

Certain alterations in the experiments mentioned above can make the findings more conclusive. Particularly, since MNPL polymers are molecules containing tens of thousands of monomer subunits, increasing the number of subunits (from the 3 unit structures used in this experiment) used in the pKa and HOMO-LUMO energy determinations would significantly improve the validity of the aforementioned procedures. Additionally, using a more accurate basis set with a more comprehensive set of theory functionals would also yield better results for the pKa and HOMO-LUMO energy values. For instance, though the pKa of ammonium is 9.25, the settings and calculations used in *Materials and Methods* approximate this value to be 36.26 (12). Though this is a significant difference, it is arduous to efficiently ascertain electron correlation energies in bigger molecules; however, this task can be hastened with increased computing power. Additionally, if an exhaustive list of chemicals that interact with the typical polypropylene/ethylene propylene diene molecule can be obtained, then instead of computing theoretical retrosynthetic routes, likely syntheses could be modeled using the same computing tool (IBM RXN for Chemistry).

5. CONCLUSION

Even though improvements can be made in the detailed procedure to assert conclusivity of functionalization plausibility and behaviors, the trends ascertained in this study– for instance, the reactivity of ethylene propylene diene and polypropylene along with plausible functionalization for the latter–should be cause for concern as MNPLs continue proliferating through different natural and industrial environments and coming in contact with various chemicals in these spaces. Particularly, special attention should be given to highly reactive plastic types, which is currently not the case in literature that tends to focus on behaviors exhibited by polystyrene microbeads. This study has revealed how even intermediate chemical species in the numerous functionalization pathways can alter polymer dipoles to favor charge-based plastic uptake, along with validating qualitative observations regarding increased uptake of aminated plastics and decreased uptake of carboxylated plastics. It should also be noted that there are many more functionalizations that were not explored in this paper that could similarly enhance uptake and increase plastic toxicity.

ACKNOWLEDGMENT

The authors would like to acknowledge Mr. Robert Gotwals and Dr. Sarah Shoemaker for facilitating study conceptualization and providing the aforementioned software packages through the NCSSM Research Experience in Computational Science (Summer Research and Innovation Program at the North Carolina School of Science and Mathematics).

REFERENCES

[1] M. O. Rodrigues, et al. Impacts of plastic products used in daily life on the environment and human health: What is known? *Environmental Toxicology and Pharmacology*. 72, 103239 (2019), https://www.sciencedirect.com/science/article/abs/pii/S1382668919300079.

[2] R. Geyer, et al. Production, use, and fate of all plastics ever made. *ScienceAdvances*. 3, 7 (2017), https://www.science.org/doi/full/10.1126/sciadv.1700782.

[3] Factora, director. How plastic is made. 2023, https://www.youtube.com/watch?v=Y7e2yHxZl3A.

[4] SkyQuest. Plastic market size & share - industry growth | 2031. 2024, https://www.skyquestt.com/report/plastic-market. Accessed 18 July 2024.

[5] J. Domenech, R. Marcos. Pathways of human exposure to microplastics, and estimation of the total burden. *Current Opinion in Food Science*. 39, 144-151 (2021), https://www.sciencedirect.com/science/article/pii/S2214799321000084.

[6] S. L. Leonard, et al. Microplastics in human blood: Polymer types, concentrations and characterisation using μFTIR. *Environment International*. 188, 108751 (2024), https://doi.org/10.1016/j.envint.2024.108751.

[7] European Chemicals Agency. Microplastics - ECHA. 2023, https://echa.europa.eu/hot-topics/microplastics. Accessed 18 July 2024.

[8] A. Banerjee, W. Shelver. Micro- and nanoplastic induced cellular toxicity in mammals: A review. Edited by D. Barcelo. *Science of the Total Environment*. 2020, pp. 1-14.

[9] J. I. Aihara. Reduced HOMO−LUMO gap as an index of kinetic stability for polycyclic aromatic hydrocarbons. *The Journal of Physical Chemistry A*. 103, 7487-7495 (1999), https://pubs.acs.org/doi/10.1021/jp990092i.

[10] E. Minikel. Organic chemistry 05: Frontier molecular orbital theory. 2015, https://www.cureffi.org/2015/02/04/organic-chemistry-05/. Accessed 18 July 2024.

[11] G. Gunawardena. Henderson-Hasselbach equation. 2022, https://chem.libretexts.org/Ancillary_Materials/Reference/Organic_Chemistry_Glossary/Henderson-Hasselbach_Equation. Accessed 18 July 2024.

[12] Study.com. Ammonium ion has a pKa of 9.25. What is the pKb for ammonia? https://homework.study.com/explanation/ammonium-ion-has-a-pka-of-9-25-what-is-the-pkb-for-ammonia.html. Accessed 18 July 2024.
[13] M. Rafi. Molecular structure of polyethylene terephthalate PET chemical formula:. Download scientific diagram. 2021, https://www.researchgate.net/figure/Molecular-Structure-of-Polyethylene-Terephthalate-PET-Chemical-Formula-C10H8O4n_fig1_351306838. Accessed 18 July 2024.
[14] Intratec Solutions. Technology profile: Production of EPDM rubber. *Chemical Engineering*. 1 April 2022, https://www.chemengonline.com/technology-profile-production-of-epdm-rubber/. Accessed 18 July 2024.
[15] J. Davidson. The monomer repeat structures of polyethylene and polypropylene, the two most commonly used synthetic polymer materials. | Download scientific diagram. https://www.researchgate.net/figure/The-monomer-repeat-structures-of-polyethylene-and-polypropylene-the-two-most-commonly_fig1_295404630. Accessed 18 July 2024.
[16] C. Shi, et al. Synthesis of aminated polystyrene and its self-assembly with nanoparticles at oil/water interface. *e-Polymers*. 2020, https://www.degruyter.com/document/doi/10.1515/epoly-2020-0038/html?lang=en.
[17] Nanjing University of Technology. Polystyrene-graft-succinic carboxylic acid resin. *Eureka*. 2010, https://eureka.patsnap.com/patent-CN101880357A.
[18] D. Jiang, C. Wilkie. Graft copolymerization of methacrylic acid, acrylic acid and methyl acrylate onto styreneâ•fiButadiene block copolymer. *e-Publications@Marquette*. 1998, https://epublications.marquette.edu/cgi/viewcontent.cgi?article=1758&context=chem_fac. Accessed 18 July 2024.
[19] J. Fallingborg. Intraluminal pH of the human gastrointestinal tract. *Danish Medical Bulletin*. 46, 183-196 (1999).
[20] Chemistry Steps. Gibbs free energy and equilibrium constant. https://general.chemistrysteps.com/gibbs-free-energy-and-equilibrium-constant/. Accessed 18 July 2024.
[21] The Engineering Toolbox. Water - ionization constant, pKw, of normal and heavy water. https://www.engineeringtoolbox.com/ionization-dissociation-autoprotolysis-constant-pKw-water-heavy-deuterium-oxide-d_2004.html. Accessed 19 July 2024.